

Managing Sets of Flying Base Stations Using Energy Efficient 3D Trajectory Planning in Cellular Networks

Mohammad Javad Sobouti, Amir Hossein Mohajerzadeh, Seyed Amin Hosseini Seno, and Halim Yanikomeroglu,
Fellow, IEEE

Abstract—Unmanned aerial vehicles (UAVs) in cellular networks have garnered considerable interest. One of their applications is as flying base stations (FBSs), which can increase coverage and quality of service (QoS). Because FBSs are battery-powered, regulating their energy usage is a vital aspect of their use; and therefore the appropriate placement and trajectories of FBSs throughout their operation are critical to overcoming this challenge. In this paper, we propose a method of solving a multi-FBS 3D trajectory problem that considers FBS energy consumption, operation time, flight distance limits, and inter-cell interference constraints. Our method is divided into two phases: FBS placement and FBS trajectory. In taking this approach, we break the problem into several snapshots. First, we find the minimum number of FBSs required and their proper 3D positions in each snapshot. Then, between every two snapshots, the trajectory phase is executed. The optimal path between the origin and destination of each FBS is determined during the trajectory phase by utilizing a proposed binary linear problem (BLP) model that considers FBS energy consumption and flight distance constraints. Then, the shortest path for each FBS is determined while taking obstacles and collision avoidance into consideration. The number of FBSs needed may vary between snapshots, so we present an FBS set management (FSM) technique to manage the set of FBSs and their power. The results demonstrate that the proposed approach is applicable to real-world situations and that the outcomes are consistent with expectations.

Index Terms—Flying base station, Trajectory optimization, Cellular networks, FSM

I. INTRODUCTION

CELLULAR networks of the next generation offer increased data transfer rates, improved service quality, and greater energy efficiency. Cellular networks, including 5G and beyond, are the backbone of future communication, capable of delivering a dependable and efficient infrastructure, resulting in a sustainable system.

Cellular networks have garnered substantial attention in recent decades and have significantly impacted human life. Due to the rapid growth in the popularity of cellular networks, communication vendors have been motivated to extend this beneficial technology and industry. For instance, the data

transmission rate of cellular networks has increased dramatically from 1.2 kbps in first-generation (1G) to 1 Gbps or higher for fifth-generation (5G) and beyond networks. As a result, 5G is expected to be a greater step in the evolution of communication technology. Both 5G and 6G technologies will benefit businesses and society in the 2030s by delivering highly reliable and secure communication services [1], [2].

Mobile user satisfaction in cellular networks depends on coverage and QoS metrics. As the quality of calls, movies, and the usage of various applications continues to increase, consumers want to enjoy this quality regardless of location, time, or circumstance, most notably on their smartphones. As a result, future generations of cellular networks' QoS and coverage must be improved. On the other hand, the increased frequencies required to serve a greater number of clients may result in coverage over a narrower region. Therefore, additional base station (BS) are required to increase the coverage area, which results in a better quality of experience (QoE) for users. Increased terrestrial base station capacity is very costly, however, and almost unattainable. With the high financial requirements of creating a new base station, assessing its location and viability for installation is exceedingly complex and expensive. Additionally, increasing the bandwidth in future generations of the cellular network reduces the base station's coverage, assuming constant antenna power. As a result, fixing this matter will need more investigation. In the meantime, FBSs offer a viable way for expanding network coverage and QoS [3], [4].

FBSs can thus be used when terrestrial base stations are uneconomical, or when they are unfeasible due to mountainous, rough, or rocky terrain. They can also be used when a cellular network is under heavy strain due to major sports or cultural events [5], [6]. FBSs are beneficial since they do not require pre-arranged equipment and almost eliminate location limits. The other desirable feature of FBSs is their increased line-of-sight (LoS), which is due to their higher placement, thereby reducing multipath fading and shadowing [7]. Additionally, because FBSs are mobile, they can improve QoS and mitigate impairments by shifting their places if the network's status deteriorates. If necessary, a mobility function can also be used to enhance the number of users covered. Additionally, users may benefit from increased data rates by expanding the coverage and number of FBSs [8].

When using FBSs in cellular networks, their placements and altitudes must be specified. Since FBSs are often battery-

MohammadJavad Sobouti, Amir Hossein Mohajerzadeh, and Seyed Amin Hosseini Seno are with the Department of Computer Engineering, Ferdowsi University of Mashhad, Mashhad,Iran, (e-mail: javad.sobouti@mail.um.ac.ir; {mohajerzadeh, hosseini}@um.ac.ir).

Halim Yanikomeroglu is with the Department of Systems and Computer Engineering, Carleton University, Ottawa, ON, Canada, (e-mail: halim@sce.carleton.ca).

The corresponding author is Amir Hossein Mohajerzadeh (email: mohajerzadeh@um.ac.ir).

powered, optimal positions and paths will extend the network's lifetime. Additionally, the locations of FBSs serving consumers are critical, as the major objective of cellular networks is to cover and deliver the level of service demanded by customers. However, because cellular users are mobile, they may move out of the range of a base station. To overcome this issue, users' positions are verified on a scheduled basis, and the location of FBSs may be identified using this information. After that, the FBSs are shifted. While FBSs can circumvent the limitations of terrestrial base stations, they face location and trajectory challenges. Numerous studies have been conducted on deploying UAVs and stations in 2D and 3D space in various wireless networks [9], [10]. Also, studies on the movement of FBSs involving wireless networks, the Internet of Things, and sensor networks have been undertaken [11], [12].

This paper considers cellular network demand in an urban area. We aim to cover users and serve their required data rate in a period of time using a 5G and beyond cellular network. In doing so, the type of FBS we consider is the DJI S900 UAV helicopter, [7] which can fly to an altitude of 3 km¹. To find the optimal trajectory of FBSs, we first must find the optimal positions of FBSs in different snapshots. We consider orthogonal frequency reuse to avoid interference between FBSs in the network, and we consider the constraint on the number of communication channels in the intracellular network. We change the proposed mathematical model in [13] to find the optimal position of FBSs in each snapshot. We consider non-line-of-sight (NLoS) path loss and aim to cover all users in each snapshot. To find the optimal trajectory of FBSs, we propose a mathematical model based on a transportation problem to minimize the total distance tracked by FBSs. We solve the proposed mathematical model for transiting FBSs between two snapshots in each step. We find the shortest path of each FBS while taking obstacles and potential collisions into account. We also consider that users may be situated at different altitudes, following a Poisson point process (PPP) distribution, with their mobility following a random waypoint. The FBSs battery and flight limitations are also considered, and we introduce an FBS set management (FSM) approach to avoid losing energy in idle hover mode and tackle the energy problem. This article provides a mathematical model and algorithms for FBSs positioning and trajectory by considering real world challenges. Following items are the contributions of this work in comparison with the studies in the literature.

- We propose a mathematical model to solve the 3D multi-FBS positioning and trajectory problems, where NLoS links and obstacles are considered. The model has a global solution (see Table I).
 - Using a Lemma, it is proved that the solution of the proposed algorithm is global and definite.
- We consider different users' altitudes (for example, in urban areas at ground level and on the upper floors

of high-rise buildings) in the positioning and trajectory problems.

- To make the problem solvable, the time is considered discrete. An efficient time period for each snapshot is calculated which is not studied in FBS trajectory field (to the best of our knowledge).
- We propose an FSM technique to avoid losing energy in idle modes. FBSs can fly to a base for recharge and come back to perform their tasks.
- We consider power consumption for the hovering and trajectory of FBSs in the proposed model. Alongside the FSM, this helps to prolong network lifetime.
- We find the shortest path for each FBS avoiding obstacles and collision with each other.

The rest of the paper is as follows. The literature is reviewed in Section II. In Section III, the system model and the channel model, is discussed. Section IV includes the problem formulation and proposed positioning and trajectory mathematical models. The proposed algorithm for solving the whole trajectory problem is presented at the end of this section. In Section V, the test system's parameters and the numerical results are discussed. Finally, the conclusion is in Section VI.

II. RELATED WORKS

Due to the high mobility, maneuverability, adaptive altitude, and low cost of FBSs, they have vital applications in wireless networks. One of the main advantages of using FBSs is that they do not need any pre-established infrastructure and can be deployed anywhere. They can also change their positions on-demand to increase coverage and QoS for users. However, the use of FBSs also has challenges, such as determining the optimal positioning, trajectory design, and number of UAVs [7], [8].

Crucial element of FBS-mounted wireless networks is trajectory design. An FBS's trajectory involves passing through several points obtained from the deployment problem. The literature on 2D and 3D positioning problems was discussed in [13], [14].

Designing an optimal trajectory is challenging because there are an unlimited number of optimization variables (e.g., UAVs' positions)² [15]. The authors of [16] proposed a single UAV to function as a mobile server, offloading computation tasks for a group of mobile users on the ground who move according to a random waypoint model. The solution they proposed aimed to aims to maximize average throughput while keeping energy consumption and customer fairness in mind, and their proposed time-saving Monte Carlo tree search (MCTS) algorithm was able to help them achieve that goal. In [17], a UAV path planning was proposed on the basis of the bat algorithm. The paper's primary goal was to enable UAVs to find a safer and shorter path without crashing through the start and end points in a war operation environment. The authors of [18] proposed a deep learning algorithm trained by a genetic algorithm (GA). The GA collected states and paths from different scenarios and then used them to train a deep neural network so that

¹Regulations generally allow UAVs to fly up to about 120 meters but sometimes more altitude is permitted. Therefore, we did not follow these restrictions in this exploratory study.

²Instead of the terms UxNB and FBS, the term most commonly used in the literature is UAV. In this section, we use these terms interchangeably.

when faced with familiar scenarios, it could quickly provide an optimized path.

In [19], a multi-UAV trajectory optimization model was proposed. The model was based on a single time interval and used time segmentation instead of traditional station segmentation, which simplified the calculation of cost functions. The authors of [20] aimed to use surveillance UAVs to compensate for the shortcomings of fixed surveillance systems, like CCTV. In [21], a secure cognitive UAV communication network was studied using the trajectory and high flexibility of a UAV and the possibility of creating direct vision links. The authors of [22] investigated the problem of safe transmission in a cache-enabled UAV relay network with device-to-device communications, assuming the presence of a listener. In [23], the authors aimed to maximize users' minimum power by optimizing the UAV trajectory and transmit power. The cache, trajectory, and transmit power optimization variables were alternatively optimized in three different blocks. The authors of [24] investigated the use of UAVs to provide a joint service to many automobiles on a highway with no infrastructure. They limited the number of UAVs installed, with limits on the required QoS, drawing on the amount of data and the influence of vehicle movement. They did this by using the optimal travel path of UAVs and assigning spectrum resources for a period of time.

In [25] the goal was to maximize system power by jointly optimizing a UAV's 3D trajectory, communication scheduling, and transmit power. In doing so, the authors first considered a specific case where the path between a UAV base station (UAV-BS) and a UAV access point (UAV-AP) is predetermined. Subsequently, they proposed an efficient iterative algorithm to optimize the 3D UAV trajectory, and this algorithm alternately optimized the sub-problems on the basis of a sequential convex approximation technique. The authors of [26] proposed an architecture of relay UAVs to load data from smartphones onto satellites in low-Earth orbit. In so doing, they improved smartphone connection time, power management, and UAV trajectory to increase network capacity. Their approach involved using non-linear integer programming (NLIP) to simulate the issue. In [27], a UAV trajectory optimization problem was formulated as a non-convex problem, which took UAV altitudes and wireless coverage performance into consideration. The authors proposed an iterative algorithm with low complexity to tackle this problem, breaking down the main problem into four sub-problems and optimizing the variables. First, a convex minimization algorithm was used to find the optimal global 2D position of the UAV. Next, the optimal altitude of the UAVs was obtained. Then, a multi-objective evolutionary algorithm based on a decomposition algorithm was proposed to control the phase of the antenna elements and achieve the desired performance. Finally, with the variables solved, the main problem was reformulated as a single-variable optimization problem, in which charging time was the optimization variable, and the problem was solved using convex optimization techniques. In [28], the focus was on UAV-enabled emergency networks, where UAVs functioned as FBSs to collect data from terrestrial users in disaster-affected areas. The energy available of the users' devices are

insufficient because of the failure of the ground power supply induced by disasters. Terrestrial impediments were also shown to impact UAV flying due to post-disaster environmental conditions. To address the issue, the authors formulated a UAV trajectory optimization problem with user-device energy constraints and the location of terrestrial obstacles to maximize the uplink efficiency of UAV networks during the flight duration. They transformed the problem into a constrained Markov decision-making process (CMDP) using the UAV as an agent because of the dynamic user-device energy constraint. They introduced a UAV path-planning algorithm based on a safe deep Q-network (safeDQN) to address the CMDP problem, in which the UAV learned to choose optimal actions on the basis of rational policies.

The authors of [29] addressed the topic of 3D UAV trajectory and spectrum allocation, considering UAV power consumption and fairness to terrestrial users. To do this, they first defined UAV power consumption as a function of 3D mobility. Then, given the restricted energy, the fair throughput was maximized. They suggested a novel Deep Reinforcement Learning-based algorithm (DRL). The proposed method allows the UAV to control its speed and direction to save energy and arrive at the target destination while still having enough energy and allocating the spectrum band to reach the fairness. In [30], a UAV was used in a wireless sensor network to collect data from multiple sensor nodes (SNs). The goal a UAV was used from SNs along with the 3D UAV trajectory. In the proposed system, the disconnection effect was also considered, and the data rate of data collection was modeled according to the communication channel. To solve the problem, the 3D motion of the path was optimized repeatedly, once horizontally and then vertically. The authors of [31] studied a UAV that sent a shared file to a set of ground terminals. Their goal was to optimize the path to minimize the UAV's mission time. The altitude was assumed to be a constant value equal to the lowest possible altitude for a safe flight. The resulting path consisted of some waypoints and extended the traveling salesman problem, except there was no need to return to the starting point. The problem was solved so that the paths were designed to meet the minimum connection time limit during which the horizontal distance between the UAV and the terminal was less than a specific value. For the given path points, the optimal speed of the UAV was obtained by solving a linear programming problem. In [32], a path for a UAV was designed to collect data from the possible sensors. The objective was to maximize the data collected using the traveling salesman problem and convex optimization. The authors of [33] examined two types of UAVs in a UAV-assisted secure network. One UAV flew about transmitting secret data to a mobile user, while the second UAV, which was there to help, made bogus noises to distract the attackers. Given the mobility of UAVs and users, the authors aimed to increase the worst-case secrecy rate of mobile users. The challenge was handled by optimizing the 3D trajectory of UAVs while taking as constraints time allocation, maximum speed, collision avoidance, placement error, and energy harvesting.

The authors of [34] jointly optimized user scheduling and

TABLE I: A comparison with existing literature

	[34]	[35]	[36]	[37]	[38]	[39]	[25]	[40]	[41]	[42]	Our work
Trajectory design	*	*			*	*	*	*	*	*	*
3D trajectory		*					*			*	*
Uplink			*	*	*		*	*	*	*	
Downlink	*						*				*
Sum-rate maximization	*			*			*		*	*	*
Energy optimization					*		*	*			*
Obstacle consideration						*					*
Time minimization		*	*	*						*	
Dynamic environment					*			*	*	*	*
Mathematical solution	*	*	*		*		*				*

UAV trajectories to maximize average data rates among ground users. They envisioned a wireless communication system where the UAVs served several ground users. The UAVs operated periodically, and each UAV had to return to the starting point at the end of each time interval. The UAV trajectories were also designed such that they respected speed limits and avoided collisions. In [35] a UAV-aided data collection is proposed to gather data from a number of ground users. The objective of the the paper is to optimize the UAV's trajectory, altitude, velocity, and data links with ground users to minimize the total mission time. The paper targets emergency applications, where the mission completion time should be the main concern. The authors of [36] considered a scenario where an UAV collects data from a set of sensors on a straight line. They considered UAV can either cruise or hover while communicating with the sensors. The objective of the paper is to minimize the UAV's total flight time from a starting point to a destination while allowing each sensor to successfully upload a certain amount of data using a given amount of energy. In [37] an on-board deep Q-network is proposed to minimize the overall data packet loss of the sensing devices. The authors have done it by optimally deciding the device to be charged and interrogated for data collection, and the instantaneous patrolling velocity of the UAV. The authors of [38] proposed a novel UAV-assisted IoT network, in which a low-altitude UAV platform is employed as both a mobile data collector and an aerial anchor node to assist terrestrial BSs in data collection and device positioning. Theirs aim is to minimize the maximum energy consumption of all devices. In [39] the state-of-the art deep reinforcement learning is merged with the UAV navigation through massive multiple-input-multiple-output (MIMO) technique to design a deep Q-network for optimizing the UAV trajectory by selecting the optimal policy. The authors of [40] considered a scenario where multiple UAVs collect data from a group of sensor nodes on the ground. They study tradeoff between the aerial cost, which is defined by the propulsion energy consumption and operation costs of all UAVs, and the ground cost, which is defined as the energy consumption of all sensor nodes. The aim is to minimize the weighted sum of the above two costs, by optimizing the UAV trajectory jointly with wake-up time allocation, as well as the

transmit power of all sensor nodes. In [41] an UAV-assisted single-hop vehicular network is considered, wherein sensors on vehicles generate time sensitive data streams, and UAVs are used to collect and process this data while maintaining a minimum age of information. The authors of [42] focused on the problem of deploying UAV-BSs to provide satisfactory wireless communication services, with the aim to maximize the total number of covered user equipment subject to user data-rate requirements and UAV-BSs' capacity limit.

The authors of [43] investigated how to construct a trajectory for a group of energy-constrained UAVs working in dynamic wireless network situations. In their model, a group of drone base stations (DBSS) was dispatched to jointly service clusters of ground users with dynamic and unexpected uplink access requests. In this scenario, the DBSSs had to maneuver together to maximize coverage for the dynamic requests of ground users. This optimization approach for trajectory design aimed to develop optimal trajectories that increased the fraction of customers served by all FBSs. A value decomposition-based reinforcement learning (VD-RL) method with a meta-training mechanism was proposed to obtain an optimal solution for this non-convex optimization problem in unpredictable situations. In [44] the objective was to minimize the average power through both the design of transmission power and the travel path for an activated network of UAVs. The authors proposed a new alternative optimization method by combining power and trajectory in an intermediate variable and then updating the power and the newly introduced variable. This new variable simplified the analysis of the main problem by turning it into two convex sub-problems, namely an operational power maximization sub-problem and a feasibility sub-problem. In [42], the authors developed a UAV-assisted IoT system that maximized the quantity of data gathered from IoT devices while depending on the UAVs' shortest flight paths. After that, a method based on deep reinforcement learning was developed to determine the best trajectory and throughput within a given coverage region. Following training, the UAV was able to gather all the data from user nodes independently, improving the overall sum rate while utilizing fewer resources. Based on a connected graph, UAV routes were designated to serve IoT devices in [45]. Their

proposed method, known as semi-dynamic mobile anchor guidance (SEDMAG), used a weighted search algorithm to determine the shortest-path energy for conservative planning to meet the nodes dynamically.

In this article, several important issues have been considered, which, to the best of our knowledge, have not been addressed independently or jointly in other related works. The most important contribution in the proposed algorithm is to provide an energy management method for FBSs, called FSM, which makes the operation time of FBSs longer and makes the problem closer to reality. In the FSM method, in each snapshot, idle FBSs return to the base and recharged so that they can be used again if needed in the future. Moreover, a method that finds the shortest possible 3D path for each FBS between any two snapshots is presented, avoiding obstacles and collisions between FBSs. In appendix, it is proved that the path is the shortest path and the optimal solution to the problem. In addition to points mentioned, we have provided a solution to find the right duration for each snapshot, which is the right time to recheck the status of network users according to the conditions of the problem. Furthermore, to find the optimal 3D positions of FBSs in each snapshot, we have presented a mathematical model with an optimal solution in the problem space, considering the path loss and the altitude of the users.

In this paper, we have tried to be the closest to the real world conditions compared to the related works. We propose an exact solution in the problem space in both positioning and trajectory phases, while taking constraints related to power consumption, data rate, interference, and FBS collision avoidance into account. Moreover, we have used mathematical model to have definite and global solution compared to heuristics or learning algorithms, which are time-consuming and do not produce an exact solution.

III. SYSTEM MODEL

In this paper, we consider a wireless cellular network in an urban environment. Users are present and gathered in different parts of the area at different times, so it is necessary to dynamically change the location of the base stations to provide the best possible services to users. Since deploying a terrestrial base station in short-term scenarios is not economically viable, we aim to offer coverage and service to all cellular users by means of FBSs. It is assumed that users in this system have different data rate needs, which we have assumed to be random on the basis of uniform distribution. Also, communication links between users and FBSs are assumed to be both LoS and NLoS. A possible assumed system is shown in Figure 1.

Our main goal in this paper is to solve a 3D trajectory planning problem for FBSs that would provide coverage and service to users with the fewest possible FBSs. To do this, we have divided the problem into several snapshots. In each snapshot, we find the most suitable 3D positions and the minimum possible number of FBSs. Then, we solve the trajectory problem to minimize the energy consumption of FBSs.

We solve the 3D positioning problem of FBSs in each snapshot based on the proposed model in [13] considering



Fig. 1: A possible scenario for the proposed system.

NLoS links and assuming 100 percent users coverage. In doing so, we find the minimum number of FBSs required on the basis of the proposed bisection algorithm. The altitude of FBSs can be assumed between the two values of H_{\min} and H_{\max} based on the characteristics of the FBSs used. In addition, different altitudes have been assumed for users in this problem, which represents the presence of users in high-rise buildings. In order to prevent inter-cell interference, we have considered the limitation of the number of internal channels in the cell.

To solve the trajectory problem, we find the shortest path between each point of origin and the destination between two consecutive snapshots while taking obstacles and the potential for collisions with FBSs into consideration. To minimize the FBSs' energy consumption, we propose a linear mathematical model based on the transportation problem between two snapshots, whereby the optimal trajectory of each FBS from origin to destination is obtained. We also assume that users move based on a random waypoint. In the following section, this will be discussed in more detail. First, however, we should introduce the communication channel between the FBS and the user.

The deployment and service of FBSs are directly related to the air-to-ground (A2G) communication links. Various models for the A2G channel have been introduced in the literature. In this paper, we use the A2G model presented in [46]. The channel model generally consists of two parts: LoS and NLoS links. The possibility of an LoS link between the FBS and the ground user is determined by several parameters, including building density, FBS location, and the elevation angle between the FBS and the ground user. In an A2G channel, the probability of an LoS link is calculated as follows:

$$P_{\text{LoS}} = \frac{1}{1 + a \exp(-b(\theta_u - a))}, \quad (1)$$

where a and b are environmental constants, and θ_u is the elevation angle between user u and the FBS, which depends on their altitudes. It is calculated as $\theta_u = \left(\frac{-180}{\pi} \tan^{-1} \frac{h_{\text{FBS}} - h_u}{d_u} \right)$, where h_{FBS} and h_u are the altitudes of FBS and user u , respectively. Also, d_u is the distance between the FBS and user u . It is calculated as $d_u = \sqrt{(x_u - x_{\text{FBS}})^2 + (y_u - y_{\text{FBS}})^2 + (h_u - h_{\text{FBS}})^2}$. It can be seen from (1) that the probability of an LoS link increases in accordance with the increasing elevation angle between the FBS and the user. The probability of having an NLoS communication link can be calculated as follows:

$$P_{\text{NLoS}} = 1 - P_{\text{LoS}}. \quad (2)$$

TABLE II: Decision variables in the positioning phase.

Decision variable	Description
x_{ij}	1, if user j is served by candidate point i , and 0, otherwise.
m_i	1, if candidate point i is selected for FBS deploying, and 0, otherwise.
h_i	The altitude of the FBS which is deployed at the candidate point i .
k_{ij}	The path loss between user j and candidate point i , if user j is served by candidate point i , and 0, otherwise.
t_{ij}	Auxiliary decision variable.

Hence, the mean path loss (in dB) for LoS and NLoS communication links can be calculated accordingly [47]:

$$L_{\text{LoS}} = 20 \log\left(\frac{4\pi f_c d_u}{C}\right) + \delta_{\text{LoS}}, \quad (3)$$

$$L_{\text{NLoS}} = 20 \log\left(\frac{4\pi f_c d_u}{C}\right) + \delta_{\text{NLoS}}, \quad (4)$$

where δ_{LoS} and δ_{NLoS} are mean losses in LoS and NLoS communication links, respectively. Also, $C = 3 \times 10^8$ is the light speed, and f_c is the carrier frequency. Therefore, the probabilistic long-term mean path loss is obtained as

$$L(d_u) = L_{\text{LoS}} \times P_{\text{LoS}} + L_{\text{NLoS}} \times P_{\text{NLoS}}. \quad (5)$$

IV. PROBLEM FORMULATION

In aiming to solve the problem of 3D trajectory planning for FBSs in a cellular network, we must find an unlimited number of continuous points for the FBSs' positions, which is an NP-hard problem [13]. To do this, we divide the problem into several snapshots and find the optimal path of FBSs between every two snapshots, taking FBS energy consumption into consideration. We divide the problem into two phases. First, we find the minimum number of FBSs required and their optimal positions in each snapshot to cover and serve users. Then, we find the optimal path of each FBS from the origin to the destination.

A. Positioning phase

In the first phase, the objective function of the positioning problem is to minimize the number of FBSs required and to find the optimal positions of FBSs to cover users. To do this, we reformulate the method proposed for FBS positioning in [13]. We consider NLoS links in this problem and aim to cover all users. We also consider FBS capacity to avoid inter-cell interference between covered users.

The decision variables considered in this formulation are presented in Table II. x_{ij} is the variable that represents whether or not user j is served by an FBS at candidate point i . m_i shows whether candidate point i is selected or not. h_i is the variable of the FBS's altitude. The path loss between user j and the FBS at candidate point i is decided by variable k_{ij} . The t_{ij} is an auxiliary decision variable. Also, the parameters used in this formulation are represented in Table III.

$$\min \sum_{i \in \mathcal{I}} \sum_{j \in \mathcal{J}} k_{ij} \quad (6a)$$

s. t

$$\sum_{i \in \mathcal{I}} x_{ij} \leq 1, \quad \forall j \in \mathcal{J}, \quad (6b)$$

$$\sum_{j \in \mathcal{J}} x_{ij} \leq \psi_{\text{FBS}}, \quad \forall i \in \mathcal{I}, \quad (6c)$$

$$x_{ij} \leq m_i, \quad \forall i \in \mathcal{I}, j \in \mathcal{J}, \quad (6d)$$

$$\sum_{i \in \mathcal{I}} \sum_{j \in \mathcal{J}} x_{ij} = U, \quad (6e)$$

$$\sum_{j \in \mathcal{J}} D_j \times x_{ij} \leq \beta \times m_i, \quad \forall i \in \mathcal{I}, \quad (6f)$$

$$\sum_{i \in \mathcal{I}} m_i = P, \quad (6g)$$

$$h_i \leq H_{\text{max}} \times m_i, \quad \forall i \in \mathcal{I}, \quad (6h)$$

$$h_i \geq H_{\text{min}} \times m_i, \quad \forall i \in \mathcal{I}, \quad (6i)$$

$$\cot(\theta) \times x_{ij} \leq \frac{h_i}{d_{ij}}, \quad \forall i \in \mathcal{I}, j \in \mathcal{J}, \quad (6j)$$

$$\begin{aligned} k_{ij} \geq & [P_{\text{LoS}} \times (4\pi \frac{f_c}{C})^2 d_{ij}^2 - h_0^2] x_{ij} \\ & + (4\pi \frac{f_c}{C})^2 \times 2 \times h_0 \times t_{ij} + x_{ij} \times 10^{\delta_{\text{LoS}}} \\ & + [P_{\text{NLoS}} \times (4\pi \frac{f_c}{C})^2 d_{ij}^2 - h_0^2] x_{ij} \\ & + (4\pi \frac{f_c}{C})^2 \times 2 \times h_0 \times t_{ij} + x_{ij} \times 10^{\delta_{\text{NLoS}}}, \end{aligned} \quad \forall i \in \mathcal{I}, j \in \mathcal{J}, \quad (6k)$$

$$k_{ij} \leq M \times x_{ij}, \quad \forall i \in \mathcal{I}, j \in \mathcal{J}, \quad (6l)$$

$$t_{ij} \leq h_i, \quad \forall i \in \mathcal{I}, j \in \mathcal{J}, \quad (6m)$$

$$t_{ij} \leq H_{\text{max}} \times x_{ij}, \quad \forall i \in \mathcal{I}, j \in \mathcal{J}, \quad (6n)$$

$$t_{ij} \geq h_i - (1 - x_{ij})H_{\text{max}}, \quad \forall i \in \mathcal{I}, j \in \mathcal{J}. \quad (6o)$$

In the proposed model, the objective function (6a) is defined to minimize the sum of path losses. Constraint (6b) stipulates that each user must be served by only one FBS. Constraint (6c) states that each FBS can serve a limited number of users based on its number of channels. Constraint (6d) shows that user j can only be served by the FBS deployed at candidate point i . Constraint (6e) stipulates that FBSs must cover all users. Constraint (6f) allows each FBS to serve its maximum data rate based on its backhaul. Constraint (6g) states that the model must select only P points from the given candidate points. Constraints (6h) and (6i) stipulate that if candidate point i is selected as the position of an FBS, the FBS must fly within the permissible range. The FBS altitude will be set to zero if the model does not select the candidate point i . Constraint (6j) prevents the assignment of users who are not in the FBS's coverage range. Constraints (6k) and (6l) are the first-order Taylor expansion of equation 4, proven in Lemma 1. In constraints (6m)–(6o) the decision variable $t_{ij} = x_{ij} \times h_i$ is used to reduce the nonlinear part to the multiplication of x_{ij} and h_i . t_{ij} must be zero if x_{ij} or h_i are equal to zero. Constraints (6m) and (6n) state this requirement. Also, t_{ij} must

be equal to h_i when x_{ij} becomes 1. Constraints (6m) and (6o) satisfy this.

Lemma 1. Consider $L(d_{ij}) = L_{\text{LoS}} \times P_{\text{LoS}} + L_{\text{NLoS}} \times P_{\text{NLoS}}$ as the path-loss function. If $L(d_{ij}) \geq \text{PL}_{\text{max}}$, then x_{ij} must be equal to 0. The statement can be rewritten as follows:

$$x_{ij} = \begin{cases} 0, & \text{if } L(d_{ij}) \geq \text{PL}_{\text{max}}, \\ 0 \text{ or } 1, & \text{otherwise.} \end{cases} \quad (7)$$

Proof. We obtain a linear conditional statement in terms of h_i by replacing $L(d_{ij})$ in (7) with its linear approximation achieved from Taylor expansion around some h_0 :

$$\begin{aligned} L(d_{ij}) &= L(h_i - h_0 + h_0) \approx L(h_0) + L'(h_0)(h_i - h_0) \\ &= [P_{\text{LoS}} \times (4\pi \frac{f_c}{C})^2 d_{ij}^2 + h_0^2] x_{ij} \\ &\quad + (4\pi \frac{f_c}{C})^2 \times 2 \times h_0 \times (h_i - h_0) + x_{ij} \times 10^{\delta_{\text{LoS}}} \\ &\quad + [P_{\text{NLoS}} \times (4\pi \frac{f_c}{C})^2 d_{ij}^2 + h_0^2] x_{ij} \\ &\quad + (4\pi \frac{f_c}{C})^2 \times 2 \times h_0 \times (h_i - h_0) + x_{ij} \times 10^{\delta_{\text{NLoS}}}. \end{aligned}$$

Now, we have

$$x_{ij} = \begin{cases} 0, & \text{if } [P_{\text{LoS}} \times (4\pi \frac{f_c}{C})^2 d_{ij}^2 + h_0^2] x_{ij} \\ & + (4\pi \frac{f_c}{C})^2 \times 2 \times h_0 \times (h_i - h_0) \\ & + x_{ij} \times 10^{\delta_{\text{LoS}}} \\ & + [P_{\text{NLoS}} \times (4\pi \frac{f_c}{C})^2 d_{ij}^2 + h_0^2] x_{ij} \\ & + (4\pi \frac{f_c}{C})^2 \times 2 \times h_0 \times (h_i - h_0) \\ & + x_{ij} \times 10^{\delta_{\text{NLoS}}}. \\ & \geq \text{PL}_{\text{max}}, \\ 0 \text{ or } 1, & \text{otherwise.} \end{cases} \quad (8)$$

Assume that $A = (4\pi \frac{f_c}{C})^2$. By simplifying the conditional expression, we have

$$x_{ij} = \begin{cases} 0, & \text{if } h_i \geq \frac{\text{PL}_{\text{max}} - (A \times (d_{ij}^2 - h_0^2) \times (P_{\text{LoS}} + P_{\text{NLoS}}))}{2Ah_0}, \\ 0 \text{ or } 1, & \text{otherwise.} \end{cases}$$

By defining $a_{ij} = \frac{\text{PL}_{\text{max}} - (A \times (d_{ij}^2 - h_0^2) \times (P_{\text{LoS}} + P_{\text{NLoS}}))}{2Ah_0}$, the conditional expression will be simplified as follows:

$$x_{ij} = \begin{cases} 0, & \text{if } h_i \geq a_{ij}, \\ 0 \text{ or } 1, & \text{otherwise.} \end{cases} \quad (9)$$

To form (9) as a valid constraint in mathematical programming, the following expression can be given:

$$x_{ij} \leq \frac{M - h_i}{M - a_{ij} + \frac{1}{2}}, \quad \forall i \in \mathcal{I}, j \in \mathcal{J}, \quad (10)$$

where M is a large number. \square

B. Trajectory phase

In the trajectory phase, our objective is to find the best path for each FBS between two snapshots while taking obstacles and the potential for collisions into account. To do so, we must first consider the interval between every two snapshots. Since the velocity of FBSs is considered constant, the time between

TABLE III: Parameters used in the positioning phase.

Parameters	Description
f_c	Carrier frequency
C	Speed of light
\mathcal{I}	Set of candidate points
\mathcal{J}	Set of users
β	FBS backhaul data rate
θ	FBS elevation angle
P	Number of FBSs to be deployed
U	Number of users
H_{min}	Minimum allowed altitude
H_{max}	Maximum allowed altitude
PL_{max}	Maximum allowed path loss in the network
ψ^{FBS}	Number of inter-cell channels
D_j	Mean data rate required by user j
d_{ij}	Distance between user j and candidate point i

every two snapshots can be also constant. According to the characteristics of the FBS, a constant speed of 15 meters per second (m/s) has been considered for the FBS. This speed is also acceptable considering the average speed of users in the urban cellular network, including fixed users, pedestrian users (with an average speed of 1 m/s), and vehicular users (with an average speed of 10 m/s). According to the (11), the Δt can be obtained on the basis of the average speed of users (Γ) and the minimum coverage range of an FBS. This means, on average, Δt seconds for a user to move out of the minimum coverage range of an FBS:

$$\Delta t = \frac{R_{\text{min}}}{\Gamma}. \quad (11)$$

The average speed of users (Γ) can also be obtained from (12). In this regard, it is assumed that $\alpha\%$ of users are stationary, $\beta\%$ are pedestrians, and $\gamma\%$ are moving in cars:

$$\Gamma = \frac{\alpha \times V_\alpha + \beta \times V_\beta + \gamma \times V_\gamma}{100}, \quad (12)$$

where V_α is equal to 0.

After finding the hovering positions where FBSs hover and serve users, we tackle the problem of calculating the best FBSs path. The purpose of this is to discover the shortest path between the origin and destination of an FBS for every two snapshots, while avoiding obstacles such as buildings. To do this, we first create a graph containing source and destination hovering points and obstacle edge points. As obstacle edges are continuous in 3D, we consider points on their edges with a fixed distance to simplify the problem while keeping generality. This distance should not be so little that the graph grows too vast, causing the problem to take too long to solve. The distance should also not be so great that it substantially impacts the solution, with the result deviating from optimal global solutions. On this point, we should note that small distances of discretizing edges (e.g., less than 5 meters) do not significantly affect the solution compared with FBSs' altitude and problem space. Then, we create each edge between two graph vertices with a cost equal to the Euclidean distance in three dimensions. In the created graph, the edge between two vertices is ignored if an obstacle splits them. Dijkstra's algorithm [48] should be used to identify the shortest paths

between every two hovering spots after the graph and edge cost have been determined. Dijkstra's algorithm is a graph traversal method that finds the shortest path between two specified vertices in a weighted graph with no negative edges. Therefore, an FBS can fly from one position to another using this graph without colliding with obstacles, as proven in Lemma 2.

Lemma 2. *In graph $G(V,E)$, when going only via visited nodes, $\text{dist}[V]$ is the shortest distance from source to V , or infinite if no such path exists. (Note that we don't assume $\text{dist}[V]$ is the shortest distance for nodes that haven't been visited.)*

Proof. The base case is when just one node is visited, namely the initial node source, in which case the hypothesis is straightforward.

Otherwise, we use the $n - 1$ visited nodes hypothesis. In such an instance, we pick an edge $V-U$ with the least $\text{dist}[U]$ of any unvisited nodes, such that $\text{dist}[U] = \text{dist}[V] + G.E[V,U]$. Because if there was a shorter way and W was the first unvisited node on that path, the original hypothesis would stipulate that $\text{dist}[W] > \text{dist}[U]$, which is a contradiction. Similarly, if there was a shorter path to U that did not use any unvisited nodes, and if the last but one node on that path was W , then $\text{dist}[U] = \text{dist}[W] + G.E[W,U]$ would be a contradiction.

After processing U , $\text{dist}[W]$ will still be the shortest distance from the source to W using only visited nodes, because if there were a shorter path that did not go through U , we would have discovered it before processing U . If a shorter path did go through U , we would have updated it when processing U .

Therefore, the shortest path from the source to node V consists only of visited nodes once all nodes have been visited; hence $\text{dist}[V]$ is the shortest distance. \square

We run the shortest path algorithm for all origin-destination points. So the shortest distance between each origin-destination pair will be found.

In formulating the problem to find the best path, as mentioned in Table IV, d_{ij} is the decision variable that must be equal to 1 if FBS i moves to position j ; otherwise, it must be equal to 0. The objective function is to minimize the total energy consumed by FBSs due to their flight (16a). E_{ij} is obtained as follows:

$$E_{ij} = \text{dist}_{ij} \times E_1 + E_U, \quad (13)$$

where E_1 is the energy consumption of the FBS for 1 meter of flying, which is calculated as

$$E_1 = \frac{\zeta \times V \times 3600}{D}, \quad (14)$$

where ζ is the battery capacity, V is the battery's voltage, and D is the total possible distance of the FBS flight. Also, $E_U = mg\Delta h$ is the potential energy consumed for FBS Δh altitude change. Therefore, E_{ij} calculated as

$$E_{ij} = (\text{dist}_{ij} \times E_1) + (mg\Delta h). \quad (15)$$

Constraint (16b) states that the model decides the path of each FBS placed in the origin snapshot. The constraint (16c)

TABLE IV: Decision variable in the trajectory phase.

Decision variable	Description
d_{ij}	1, if FBS i moves to position j in the next snapshot, and 0; otherwise.

TABLE V: Parameters used in the trajectory phase.

Parameters	Description
E_{ij}	The energy that the FBS consumes to fly between position i and position j
\mathcal{M}	Set of origin FBS positions
\mathcal{N}	Set of destination FBS positions
$\text{Energy}_{\text{th}}$	Minimum required energy for an FBS to fly to the base
dist_{ij}	The distance between position i and position j
$\text{Distance}_{\text{th}}$	Maximum allowed distance that the FBS can fly between two snapshots

ensures that each position in the subsequent snapshot is chosen for one FBS. \mathcal{M} and \mathcal{N} are sets of FBS positions in the origin and destination snapshots, respectively. The size of each set is twice the maximum required FBSs to ensure that the mathematical model has a feasible solution in every iteration. (16d) is the constraint of the FSM; when the number of FBSs required in one snapshot is less or more than another, extra FBSs are moved to or from the base to save their energy, recharge, or extend the network coverage. The concept of FSM is similar to that of cell switch-off (CSO). Constraint (16e) ensures that each FBS has enough power to fly to the next position. $\text{Energy}_{\text{th}}$ is the minimum energy required for each FBS to fly to the base. If an FBS does not have enough power to continue serving users, the d_{ij} variable will choose the path to the base. The FBS will return to the base, and the other FBS will be used to fly from the base to the destination point. We call this process FSM:

$$\min \sum_{i \in \mathcal{M}} \sum_{j \in \mathcal{N}} d_{ij} \times E_{ij} \quad (16a)$$

s.t

$$\sum_{j \in \mathcal{N}} d_{ij} = 1, \quad \forall i \in \mathcal{M}, \quad (16b)$$

$$\sum_{i \in \mathcal{M}} d_{ij} = 1, \quad \forall j \in \mathcal{N}, \quad (16c)$$

$$\sum_{i \in \mathcal{M}} \sum_{j \in \mathcal{N}} d_{ij} = \max(\mathcal{M}, \mathcal{N}), \quad (16d)$$

$$d_{ij} \times E_{ij} \leq \text{Energy}_{\text{th}}, \quad \forall i \in \mathcal{M}, j \in \mathcal{N}, \quad (16e)$$

$$d_{ij} \times \text{dist}_{ij} \leq \text{Distance}_{\text{th}}, \quad \forall i \in \mathcal{M}, j \in \mathcal{N}. \quad (16f)$$

Constraint (16f) states that no FBS can fly further than its threshold distance based on its constant velocity. The $\text{Distance}_{\text{th}}$ parameter is derived as follows:

$$\text{Distance}_{\text{th}} = V_{\text{FBS}} \times \Delta t, \quad (17)$$

where Δt is the time interval between two snapshots. The trajectory parameters are described in Table V.

The total energy of the path for each FBS (E_{path}) is obtained as follows:

$$E_{\text{path}} = E_{ij} + E_{\text{hover}}, \quad (18)$$

where E_{hover} is the energy consumed when the FBS hovers. In Theorem presented in appendix A, we prove that the obtained path considering obstacles is the global shortest path possible for each FBS.

C. FSM

After finding the path energy (E_{path}) of each FBS for each subsequent snapshot, we must check if the energy of each FBS is enough to fly to the destination through the selected path. Suppose the remaining energy of the FBS after flying to the destination is less than $\text{Energy}_{\text{th}}$, or the number of required FBSs in the subsequent snapshot is less than the current snapshot. In that case, some FBSs must return to the base to recharge and wait. Moreover, if in the subsequent snapshot more FBSs are needed, the FBSs required must fly to the selected destination points through the selected paths. This whole process is called FSM

As a general solution to the entire problem, we carry out the following steps. First, we divide the problem into several snapshots. In each snapshot, users may have different positions and data rate demands. In each snapshot, we solve the 3D positioning problem to find the minimum number of required FBSs and their proper positions. Then, we create a graph based on origin and destination hovering points and obstacle edge points. After that, we find the shortest path between each origin-destination pair while taking obstacles into consideration. As Theorem 1 proves, the probability of an FBS colliding is almost zero. Next, we solve the trajectory problem between two snapshots in a row using the proposed mathematical model and updating the FBSs energy parameter considering trajectory and hovering power consumption. The proposed trajectory model decides the best path for each FBS to minimize the total energy consumption. It also decides whether an FBS should return to base due to a lower number of required FBS or due to the need to recharge batteries (concept FSM). Both proposed mathematical models are in linear form. The proposed positioning model is a mixed-integer linear problem (MILP), and the proposed trajectory model is a binary linear problem (BLP). Also, Dijkstra's algorithm has an exact solution. Therefore, the proposed method reaches the exact solution. The process continues until there is no remaining snapshot. The whole process is shown in Algorithm 1.

Theorem 1. *The probability of an FBS colliding is almost zero.*

Proof. We know that infinite lines can be drawn in 3D. Therefore, the probability of finite lines colliding is almost zero (1). Also, since the origin and destination points of neither of the two FBS paths in the proposed deployment model are equal, there are no two paths that originate from one point (2). If the destination point of one path intersects with the origin point of another, since the second FBS had moved before and changed its position, the first FBS will not collide with the second FBS at the end of its path (3). In addition, if two FBS paths collide and only if the intersection point is at the same distance from the origin point of each FBS (assuming the speed of both FBSs is constant and equal), then the FBSs

Algorithm 1 The FSM algorithm

- Solve the positioning problem in s_0 snapshot and find the number of required FBSs (\mathcal{M})
 - Calculate Δt using eq. 11
 - while** there is remaining snapshot **do**
 - Solve the positioning problem in i -th snapshot (s_i) and find the number of required FBSs (\mathcal{N})
 - Create graph $G(V, E)$
 - Find the shortest path between every origin-destination pair from \mathcal{M} and \mathcal{N} considering collisions
 - Calculate $\text{Distance}_{\text{th}}$ using eq. 17
 - Solve the proposed mathematical model for trajectory using \mathcal{M} and \mathcal{N}
 - Update FBSs remaining energy
 - if** an FBS landed in the base **then**
 - recharge it
 - end if**
 - $\mathcal{M} \leftarrow \mathcal{N}$
 - end while**
-

will collide with each other. The probability of this event is almost zero, and by taking turns in the movement of FBSs, this event can also be prevented (4).

By taking 1, 2, 3, and 4 into consideration, we can conclude that the probability of a collision between the two FBSs in the proposed model is almost zero. \square

V. NUMERICAL RESULTS

In this section, we first introduce the test system and simulation parameters. We then discuss and compare the results of scenarios for the 3D FBS trajectory problem.

A. Test system

In the simulations, we consider a centralized decision-making system for FBSs positioning and trajectory. Referring to [47] and [49], as mentioned in Table VI, we consider a $5,000 \times 5,000$ meter urban area with scenarios including 80, 200, and 450 users with Poisson point process (PPP) distribution. The PPP parameter $\lambda = 20,000$, and the environment parameters are as follows: $f_c = 2$ GHz, $\text{PL}_{\text{max}} = 110$ dB, and $(a, b, \delta_{\text{LoS}}, \delta_{\text{NLoS}}) = (9.61, 0.16, 1, 20)$, corresponding to urban environments. Additionally, we consider that the data rate requested by users has a uniform distribution with a maximum value of 6 Mbps ($D_{\text{avg}} = 3$ Mbps). The FBSs' backhaul data rate (β) is considered equal to 100 Mbps for each. The FBSs' flying altitude range is between 110 and 600 meters, and users may be situated anywhere from 0 to 150 meters, as we consider the maximum obstacle height to be 150 meters. The minimum building height is considered to be 30 meters. Moreover, we assumed that there are 25 high-rise buildings in the area. The distance between each two edge points of buildings is also considered equal to 10 meters. The capacity of the FBSs' battery (ζ) is considered 15,000 mAh. In addition, we assume the maximum distance (D) that one FBS can fly with this battery to be 15 km. We also consider the FBS's hovering energy consumption to be equal to 1,000

TABLE VI: Test parameters to evaluate the problem model.

Parameters	Description
<i>Region</i>	$5,000 \times 5,000$ m
U	80, 200, 450
β	100 Mbps
D_{avg}	3 Mbps
H_{min}, H_{max}	110 m, 600 m
BH_{min}, BH_{max}	30 m, 150 m
B_{number}	25
Distance between edge points	10 m
f_c	2 GHz
PL_{max}	110 dB
a	9.61
b	0.16
δ_{LoS}	1
δ_{NLoS}	20
V_{FBS}	15 m/s
ζ	15,000 mAh
D	15 km
$Battery_v$	11.1 v
E_{hover}	1,000 J

joules [7]. The battery assumed in this article for each FBS is a 3-cell type, and its output voltage ($Battery_v$) is assumed to be 11.1 volts. We also consider 45 degrees to be the elevation angle of FBSs. We use the Merge cell method proposed in [13] for the positioning model to find candidate points. We also used the Cplex solver to solve the positioning and trajectory mathematical models. We ran the simulation and solved the models many times; the results of the simulation are presented below.

B. Results

In the following, we discuss the results of the proposed positioning and trajectory approach, compare the results of three different numbers of users.

The number of required FBSs for each scenario with different methods is illustrated in Figure 2. The proposed FSM method is compared with the ordered artificial bee colony (ABC)-based placement (OAP) and QoS-GA methods. In the OAP algorithm, by grouping users into several groups, the service users of each UAV were first identified. One UAV serves each group of users. Then, each UAV's 3D position was chosen based on the clustering criteria [10]. QoS-GA is a GA-based FBSs deployment technique which has been developed to maximize the number of covered UEs while also satisfying

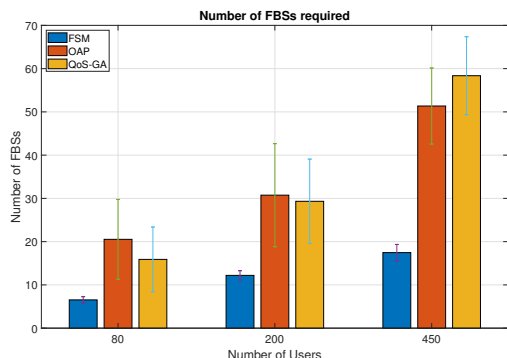
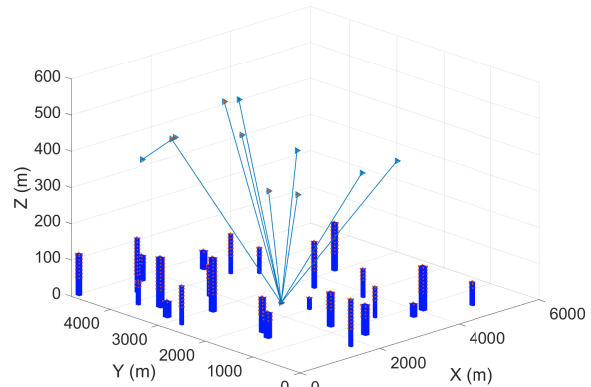
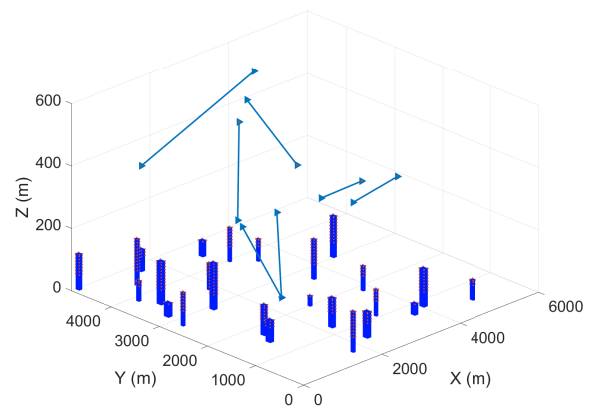


Fig. 2: Comparison of FBSs required for different methods.



(a) FBS trajectories phase 1.



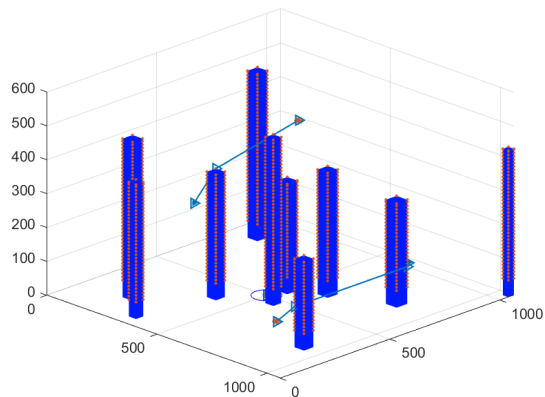
(b) FBS trajectories phase 2.

Fig. 3: FBSs trajectories in two subsequent snapshots in the 80-user scenario.

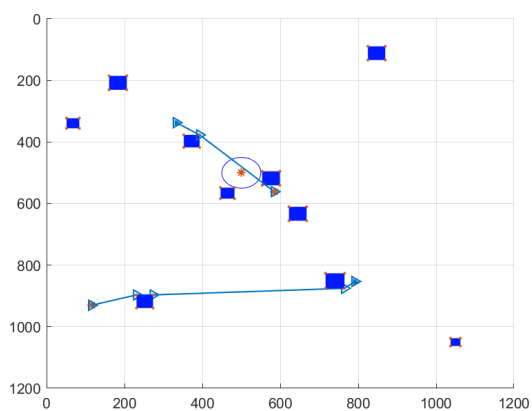
their data rate needs within the FBSs' capacity constraint. The population size, crossover rate, and mutation rate are three variables that affect the fundamental GA process. The number of potential solutions depends on the size of the population. The crossover rate and mutation rate values reflect the variety of potential solutions throughout an iteration. Up until the time step hits an iteration limit, the entire process is repeated. The GA model treats each FBS's horizontal location and coverage radius as a gene. Some iterations are then run to determine the 2D deployment outcome [49].

As we can see, the proposed method needs fewer FBSs to cover all users in different scenarios. In the proposed FSM method, on average, for 80 users, about 6 FBSs are needed to cover all users in each snapshot. For 200 and 450 users, on average, about 12 and 17 FBSs are needed, respectively.

Each snapshot is 15 seconds away from the next one, and between each two positioning snapshots, a trajectory problem is solved. Figure 3 shows the FBSs trajectories in two different snapshots. In Figure 3a, it is shown that FBSs fly from red points to blue points. Some of them increases its altitude while others does the opposite. This happens because some users move to different positions and a group of them may



(a) FBS trajectories and obstacle avoidance - 3D view.



(b) FBS trajectories and obstacle avoidance - 2D view.

Fig. 4: FBSs trajectories and their obstacle avoidance.

become very dense. Also, since the power of some of FBSs is not enough to continue their mission, the FBSs which were operated in the last snapshot returned to the base, and the two alternative full-power FBSs flew to the red points to operate. In addition, the two FBSs that returned to the base will be recharged for further missions. Moreover, as we need fewer FBSs than the previous snapshot, the extra FBSs that returned to the base will recharge and wait for future missions. Figure 3b illustrates that in this snapshot we need two more FBSs to cover users. Therefore, two new FBSs fly from the base to the destination points. The power of the last two FBSs is not enough for the next operation. All of these trajectories are designed taking obstacles and collision avoidance into consideration.

A scenario of how two FBSs move inside the target area is presented 3D in Figure 4a and 2D in Figure 4b. Both Figures illustrate the trajectory within a snapshot from t_1 to t_2 . FBSs move from their origin to the destination during the snapshot avoiding obstacles by applying the proposed algorithm. It is worth mentioning that the path used by FBSs is the shortest possible path between the origin and the destination which is presented in 2D and 3D. Red dot in 4 illustrates the place of the base where FBSs can recharge.

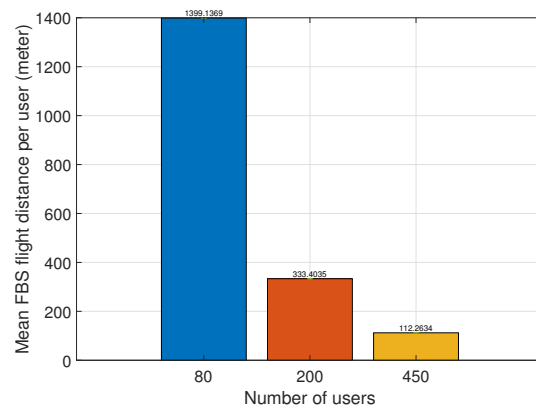


Fig. 5: Mean FBS flight distance per user.

Figure 5 presents a comparison of the mean FBS flight distance per user during the FBS operations. As the number of users increases, because we have more FBSs, the mean flight distance of an FBS decreases. When we have fewer FBSs, the total distance of FBSs will increase.

In Figure 6, the average FBS flight energy consumption is compared in different scenarios. Energy includes the hovering and trajectory power consumed. As expected, with the increase in the number of users, the average power consumption of each FBS must decrease because of shorter paths for FBSs and, therefore, less recharging. For example, with 80 users, the number of FBSs is fewer than in other scenarios. As the mean flight distance of each FBS is greater, the mean energy consumption of each FBS is more significant than in other scenarios.

Figure 7 shows the comparison of the average solving time of the trajectory problem. As we can see, besides the proposed trajectory mathematical model having an exact solution, the time it takes to solve the problem is less than the time interval between two snapshots. It means we have enough time to solve the problem in the real world. By the way, we might add that a greater number of FBSs will mean more time to solve the problem. However, sometimes to have the optimum solution of the problem and minimize the FBSs energy consumption

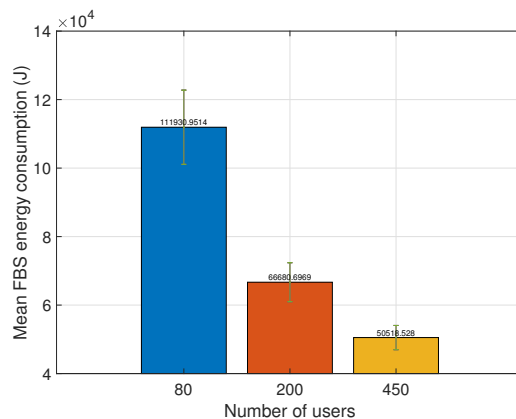


Fig. 6: Mean FBS energy consumption.

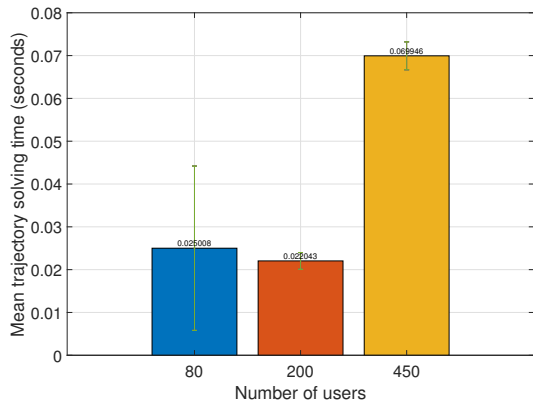


Fig. 7: Mean trajectory solving time.

considering the constraints of the problem, the solving time can increase. As the figure shows, the average time it takes to solve the 80-user scenario is somewhat longer than the 200-user scenario because of some data calculations. It is worth noting that the standard deviation of trajectory solving time with 80 users shows that in some cases, the solving time of this scenario is less than the minimum solving time of other scenarios.

Figure 8 shows that with an increasing number of users, the mean data rate served by each FBS increases. Therefore, we can conclude that the backhaul's efficiency will increase with a greater number of users, and more backhaul will be used in each small cell during the operation.

Figure 9 presents the throughput of the proposed algorithm compared with [42]. The algorithm of [42] is selected because it uses RL based algorithm for trajectory. We have proved the efficiency of the proposed algorithm in 2; this evaluation is used as a verification for the claim. Using the mean of achieved throughput in several runs, throughput of the proposed algorithm is 57 and 34 for 2. The minimum achieved throughput of the proposed algorithm in several runs is more than the maximum achieved throughput of 2. It is worth mentioning that 2 uses only one FBS, does not consider obstacles, does not consider energy, and does not report its processing and

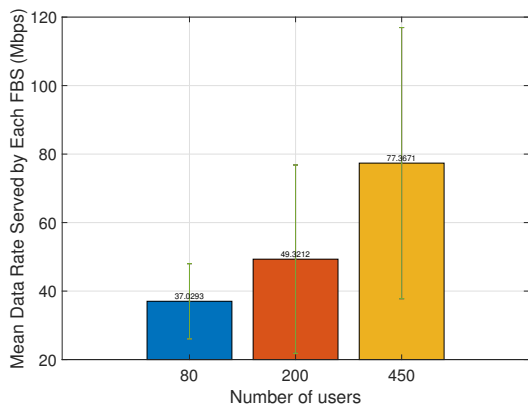


Fig. 8: Mean data rate served by each FBS.

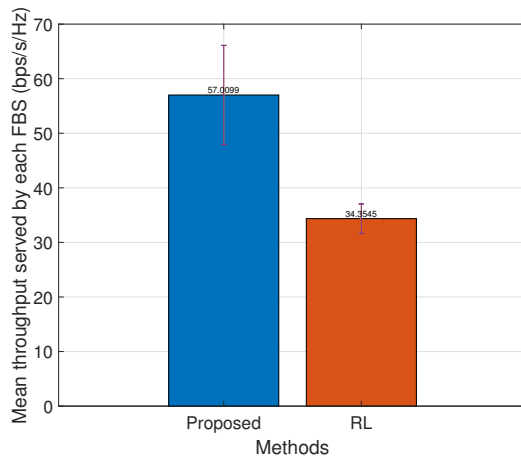


Fig. 9: Comparison of throughput of RL [42] and proposed method.

train time. We have reported the energy consumption in 6 and processing time in 7. The proposed algorithm achieves better result despite it uses more real-world characteristics. There are 40 users in a

VI. CONCLUSION

This paper proposed an approach with an exact solution for the problem of multiple 3D trajectories for FBSs, while considering constraints related to energy consumption, operational time, flight distance, inter-cell interference, and collision avoidance. The approach consisted of two phases, namely an FBS positioning phase and an FBS trajectory phase, where we divided the problem into several snapshots. First, we found the minimum number of FBSs required along with their optimal 3D positions in each snapshot. Then, the trajectory phase ran between every two snapshots. The optimum path between the origin and the destination in the trajectory phase was found using the proposed binary linear problem (BLP) model, considering FBS energy consumption and flight distance limitations. As the proposed method was a BLP, the solution was the optimal one. We used a shortest path heuristic to find the best path of each FBS from origin to the destination, taking the constraint of collision avoidance into account. In different snapshots, the required number of FBSs could be different. To address this, we introduced the FSM approach to manage the set of FBSs and their power. The results showed that the proposed method is operational in real-world scenarios. The results also showed that the mean FBS flight distance per user and mean FBS energy consumption decreased as the number of users increased. Also, the mean data rate served by each FBS was shown to increase as the number of users increased.

APPENDIX

The proof for the global and definite solution of the proposed algorithm

Theorem 2. *Suppose there is no direct path between points A and B (the connecting line between A and B passes through an obstacle), then the path obtained from the proposed algorithm*

based on the proposed graph and Dijkstra's algorithm will be the shortest path from A to B.

Proof. There are two cases for the problem, 1) where the path only passes one vertex of the obstacle, and 2) where the path passes two vertexes of the obstacle. We will provide a proof for the theorem for each case in the following.

1) The path only passes one vertex of the obstacle, from point A to M and from M to B.

This case includes two sub-cases which will be presented in 1-a and 1-b. 1-a) In this sub-case, as you can see in Figure 10, if a curved path from point A (source) to B (destination) exists, the shortest path would be a path that passes point M (vertex of the obstacle).

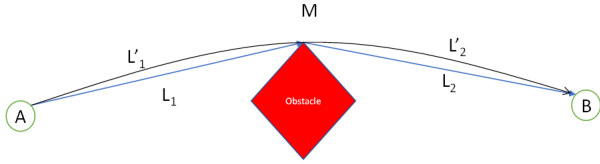


Fig. 10: Proof for case 1-a, where there is curved line, presenting point M.

To illustrate the proof, we assume that there is another curved path from A to B that passes a point N as shown in Figure 11.

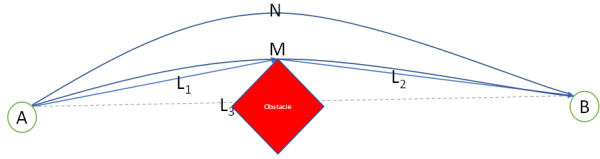


Fig. 11: Proof for case 1-a, where there is curved line, presenting point N.

We consider the line between A and B as the axis of a coordinate plane, so the area under the curved line passes point N is more than the area under the curved line passes point M. The area under the curved line L is calculated as follows:

$$L = \int_A^B \sqrt{1 + [f'(x)]^2} dx. \quad (19)$$

Since point M is closer to the axis than N (the curved line can not pass through the obstacle), we have $\int_A^B f_M(x) dx < \int_A^B f_N(x) dx$. Therefore the shortest curved line passes point M. Noting that the curved line from A to M (L'_1) is longer than the straight line from A to M (L_1) and the curved line from M to B (L'_2) is longer than the straight line from M to B (L_2), therefore, the curved line from A to B ($L'_1 + L'_2$) is longer than the straight line from A to M and then from M to B ($L_1 + L_2$). Since the point N is an arbitrary point, we can reason that every other path from A to B is longer than the path that passes M.

1-b) In the other sub-case, as shown in Figure 12, we assume that there is a straight line from A to N (L'_1) and then from N to B (L'_2).

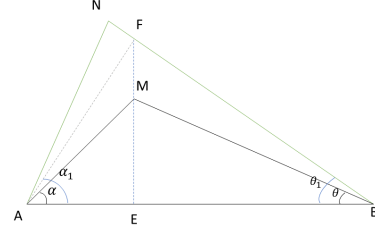


Fig. 12: Proof for case 1-b, where there is straight line, presenting point M and N.

where $\theta < \theta_1 \rightarrow \cos \theta > \cos \theta_1 \rightarrow \frac{BE}{BM} > \frac{BE}{BF} \rightarrow BF > BM$.

Now, to achieve the goal, we have to prove that $FN + NA > AM$. According to "Triangle Sides Inequality Theorem" we have $AF < AN + NF$. Similar to the fact $\theta < \theta_1$ we have $\alpha < \alpha_1$, which leads to know $AF > AM$. As a result we will have:

$$(AF < AN + NF, AF > AM) \rightarrow AN + NF > AM. \quad (20)$$

1-b') The sub-case 1-b, can also be proved in the following way:

As shown in 13, since the bases of the two triangles T and T' are equal (the straight line from A to B (L_3)), and also considering that no path from A to the hypothetical point N and from N to B can cross the obstacle, it can be concluded that $h < h'$, as a result, the area of triangle T is less than the area of triangle T'.

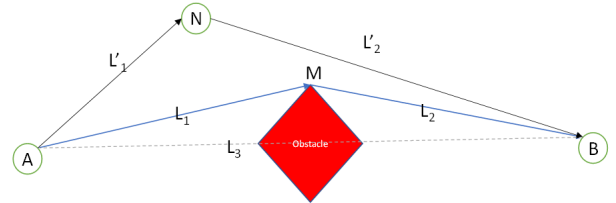


Fig. 13: Another proof for case 1-b.

According to these assumptions, based on Heron's theorem, it can be proved that for T triangle

$$A_T = \sqrt{S_T(S_T - L_1)(S_T - L_2)(S_T - L_3)}, \quad (21)$$

where $S_T = \frac{L_1 + L_2 + L_3}{2}$. Also for T' triangle

$$A_{T'} = \sqrt{S_{T'}(S_{T'} - L'_1)(S_{T'} - L'_2)(S_{T'} - L_3)}, \quad (22)$$

where $S_{T'} = \frac{L'_1 + L'_2 + L_3}{2}$.

According to A_T and S_T , the A_T can be obtained as follows:

$$A_T = 0.25 * \sqrt{(L_1^2 + L_2^2 + L_3^2)^2 - 2(L_1^4 + L_2^4 + L_3^4)}. \quad (23)$$

Since $A_T < A'_T$, so we need to prove the correctness of (24) and (25).

$$(L_1^2 + L_3^2 + L_3^2)^2 < (L_1'^2 + L_3'^2 + L_3^2)^2, \quad (24)$$

$$-2(L_1^4 + L_2^4 + L_3^4) > -2(L_1'^4 + L_2'^4 + L_3^4). \quad (25)$$

In (24), considering that L_3 is common and equal in both triangles, as a result $(L_1^2 + L_2^2)^2 < (L_1'^2 + L_2'^2)^2$. So $L_1^2 + L_2^2 < L_1'^2 + L_2'^2$. Since the length of the triangle is always a positive value,

$$L_1 + L_2 < L_1' + L_2'. \quad (26)$$

We can draw conclusions for (25) as well,

$$(L_1^4 + L_2^4 + L_3^4) < (L_1'^4 + L_2'^4 + L_3^4). \quad (27)$$

Since L_3 is common to both triangles and the length of the sides is always positive, we can also conclude from (27) that $L_1 + L_2 < L_1' + L_2'$. As a result, the path passing through the edge of the obstacle is the shortest possible path from A to B.

2) The path passes two vertexes of the obstacle, from point A to M_1 , from M_1 to M_2 and then from M_2 to B.

In this case, it will be proved for each of the triangles AM_1M_2 and M_1M_2B that they present the shortest path, likewise the proof 1. Now, we have to prove that for any arbitrary point N, the path passing N, will be longer than path mentioned in this case passing two vertexes.

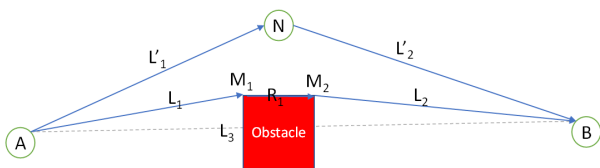


Fig. 14: Proof for case 2, where there is straight line, presenting point N.

As presented in 14, knowing the fact that straight line from point A to M_1 is shortest path from A to the vertex of the obstacle (M_1), if the length of the straight line from A to N is shorter than the straight line from A to M_1 , or similarly, if the length of the straight line from N to B is shorter than the straight line from M_2 to B, the path passing N hits the obstacle or it is tangent to either the straight line from A to M_1 or the straight line from M_2 to B as presented in 15.

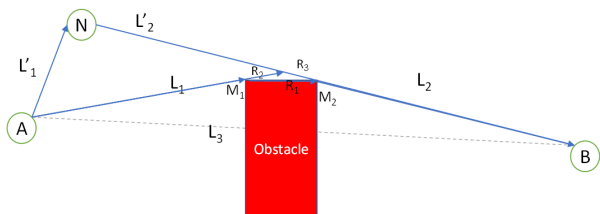


Fig. 15: Proof for case 2, presenting the contradiction of the path passing point N.

If one of the paths is tangent, according to "Triangle Sides Inequality Theorem", $L_1 + R_2 < L_1' + L_2'$ and since $R_1 <$

$R_2 + R_3$ then $R_1 - R_2, R_3$. Therefore $L_1 + R_1 < L_1' + L_2' + R_3$. Now, it is concluded that the length of every path from A to N that does not pass M_1 is longer than the path the passes M_1 based on the "Triangle Sides Inequality Theorem". Similarly, the path from N to B must pass M_2 as depicted in 16.

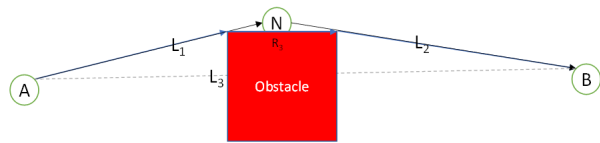


Fig. 16: Proof for case 2, presenting the contradiction of the path passing point N where one or more lines are tangent.

Knowing the fact that the path including A, N, B must be rewritten as A, M_1 , N, M_2 , B; according to the "Triangle Sides Inequality Theorem" the A, N, B path could not be shorter than A, M_1 , M_2 , B path. Therefore, the path that passes the vertexes is the shortest. \square

REFERENCES

- [1] X. Foukas, G. Patounas, A. Elmokashfi, and M. K. Marina, "Network Slicing in 5G: Survey and Challenges," *IEEE Communications Magazine*, vol. 55, no. 5, pp. 94–100, May 2017.
- [2] K. Sheth, K. Patel, H. Shah, S. Tanwar, R. Gupta, and N. Kumar, "A Taxonomy of AI Techniques for 6G Communication Networks," *Computer Communications*, vol. 161, no. 1, pp. 279–303, Sep. 2020.
- [3] I. Bekmezci, O. K. Sahingoz, and Ş. Temel, "Flying Ad-hoc Networks (FANETs): A Survey," *Ad Hoc Networks*, vol. 11, no. 3, pp. 1254–1270, May 2013.
- [4] S. Hayat, E. Yanmaz, and R. Muzaffar, "Survey on Unmanned Aerial Vehicle Networks for Civil Applications: A Communications Viewpoint," *IEEE Communications Surveys & Tutorials*, vol. 18, no. 4, pp. 2624–2661, Fourthquarter 2016.
- [5] E. Kalantari, M. Z. Shakir, H. Yanikomeroglu, and A. Yongacoglu, "Backhaul-aware Robust 3D Drone Placement in 5G+ Wireless Networks," in *Proceeding of 2017 IEEE International Conference on Communications Workshops (ICC Workshops)*, pp. 109–114.
- [6] M. Alzenad, A. El-Keyi, F. Lagum, and H. Yanikomeroglu, "3-D Placement of an Unmanned Aerial Vehicle Base Station (UAV-BS) for Energy-efficient Maximal Coverage," *IEEE Wireless Communications Letters*, vol. 6, no. 4, pp. 434–437, Aug. 2017.
- [7] A. Fotouhi, H. Qiang, M. Ding, M. Hassan, L. G. Giordano, A. Garcia-Rodriguez, and J. Yuan, "Survey on UAV Cellular Communications: Practical Aspects, Standardization Advancements, Regulation, and Security Challenges," *IEEE Communications Surveys & Tutorials*, vol. 21, no. 4, pp. 3417–3442, Fourthquarter 2019.
- [8] M. Mozaffari, W. Saad, M. Bennis, Y.-H. Nam, and M. Debbah, "A Tutorial on UAVs for Wireless Networks: Applications, Challenges, and Open Problems," *IEEE Communications Surveys & Tutorials*, vol. 21, no. 3, pp. 2334–2360, Thirdquarter 2019.
- [9] Y. Sun, T. Wang, and S. Wang, "Location Optimization and User Association for Unmanned Aerial Vehicles Assisted Mobile Networks," *IEEE Transactions on Vehicular Technology*, vol. 68, no. 10, pp. 10,056–10,065, Oct. 2019.
- [10] C. Zhang, L. Zhang, L. Zhu, T. Zhang, Z. Xiao, and X.-G. Xia, "3D Deployment of Multiple UAV-mounted Base Stations for UAV Communications," *IEEE Transactions on Communications*, vol. 69, no. 4, pp. 2473–2488, Apr. 2021.
- [11] B. Khamidehi and E. S. Sousa, "Trajectory Design for the Aerial Base Stations to Improve Cellular Network Performance," *IEEE Transactions on Vehicular Technology*, vol. 70, no. 1, pp. 945–956, Jan. 2021.
- [12] W. Shi, J. Li, N. Cheng, F. Lyu, S. Zhang, H. Zhou, and X. Shen, "Multi-drone 3-D Trajectory Planning and Scheduling in Drone-assisted Radio Access Networks," *IEEE Transactions on Vehicular Technology*, vol. 68, no. 8, pp. 8145–8158, Aug. 2019.
- [13] Z. Rahimi, M. Sobouti, R. Ghanbari, S. A. Hosseini Seno, A. Mohajerzadeh, H. Ahmadi, and H. Yanikomeroglu, "An Efficient 3D Positioning Approach to Minimize Required UAVs for IoT Network Coverage," *IEEE Internet of Things Journal*, vol. 9, no. 1, pp. 558–571, Jan. 2022.

- [14] M. J. Sobouti, Z. Rahimi, A. H. Mohajerzadeh, S. A. Hosseini Seno, R. Ghanbari, J. M. Marquez-Barja, and H. Ahmadi, "Efficient Deployment of Small Cell Base Stations Mounted on Unmanned Aerial Vehicles for the Internet of Things Infrastructure," *IEEE Sensors Journal*, vol. 20, no. 13, pp. 7460–7471, Feb. 2020.
- [15] Y. Zeng, R. Zhang, and T. J. Lim, "Wireless Communications With Unmanned Aerial Vehicles: Opportunities and Challenges," *IEEE Communications Magazine*, vol. 54, no. 5, pp. 36–42, May 2016.
- [16] Y. Qian, K. Sheng, C. Ma, J. Li, M. Ding, and M. Hassan, "Path Planning for the Dynamic UAV-Aided Wireless Systems using Monte Carlo Tree Search," *IEEE Transactions on Vehicular Technology*, Mar. 2022.
- [17] X. Zhou, F. Gao, X. Fang, and Z. Lan, "Improved Bat Algorithm for UAV Path Planning in Three-dimensional Space," *IEEE Access*, vol. 9, pp. 20 100 – 20 116, Jan. 2021.
- [18] Y. Pan, Y. Yang, and W. Li, "A Deep Learning Trained by Genetic Algorithm to Improve the Efficiency of Path Planning for Data Collection With Multi-UAV," *IEEE Access*, vol. 9, pp. 7994–8005, 2021.
- [19] Q. Xia, S. Liu, M. Guo, H. Wang, Q. Zhou, and X. Zhang, "Multi-UAV Trajectory Planning Using Gradient-based Sequence Minimal Optimization," *Robotics and Autonomous Systems*, vol. 137, p. 103728, Mar. 2021.
- [20] Y. Tang, Y. Miao, A. Barnawi, B. Alzahrani, R. Alotaibi, and K. Hwang, "A Joint Global and Local Path Planning Optimization for UAV Task Scheduling Towards Crowd Air Monitoring," *Computer Networks*, vol. 193, p. 107913, Jul 2021.
- [21] Y. Zhou, F. Zhou, H. Zhou, D. W. K. Ng, and R. Q. Hu, "Robust Trajectory and Transmit Power Optimization for Secure UAV-enabled Cognitive Radio Networks," *IEEE Transactions on Communications*, vol. 68, no. 7, pp. 4022–4034, Jul. 2020.
- [22] J. Ji, K. Zhu, D. Niyato, and R. Wang, "Joint Trajectory Design and Resource Allocation for Secure Transmission in Cache-enabled UAV-relaying Networks with D2D Communications," *IEEE Internet of Things Journal*, vol. 8, no. 3, pp. 1557 – 1571, Feb. 2021.
- [23] —, "Joint Cache Placement, Flight Trajectory and Transmission Power Optimization for Multi-UAV Assisted Wireless Networks," *IEEE Transactions on Wireless Communications*, vol. 19, no. 8, pp. 5389 – 5403, Aug. 2020.
- [24] M. Samir, S. Sharafeddine, C. Assi, T. M. Nguyen, and A. Ghayeb, "Trajectory Planning and Resource Allocation of Multiple UAVs for Data Delivery in Vehicular Networks," *IEEE Networking Letters*, vol. 1, no. 3, pp. 107–110, May 2019.
- [25] M. Hua, L. Yang, Q. Wu, and A. L. Swindlehurst, "3D UAV Trajectory and Communication Design for Simultaneous Uplink and Downlink Transmission," *IEEE Transactions on Communications*, vol. 68, no. 9, pp. 5908–5923, Sep. 2020.
- [26] Y. Wang, Z. Li, Y. Chen, M. Liu, X. Lyu, X. Hou, and J. Wang, "Joint Resource Allocation and UAV Trajectory Optimization for Space-Air-Ground Internet of Remote Things Networks," *IEEE Systems Journal*, vol. 15, no. 4, pp. 4745–4755, Dec. 2021.
- [27] W. Feng, N. Zhao, S. Ao, J. Tang, X. Y. Zhang, Y. Fu, D. K. So, and K. K. Wong, "Joint 3D Trajectory Design and Time Allocation for UAV-Enabled Wireless Power Transfer Networks," *IEEE Transactions on Vehicular Technology*, vol. 69, no. 9, pp. 9265–9278, Sep. 2020.
- [28] T. Zhang, J. Lei, Y. Liu, C. Feng, and A. Nallanathan, "Trajectory Optimization for UAV Emergency Communication with Limited User Equipment Energy: A Safe-DQN Approach," *IEEE Transactions on Green Communications and Networking*, vol. 5, no. 3, pp. 1236–1247, Sep. 2021.
- [29] R. Ding, F. Gao, and X. S. Shen, "3D UAV Trajectory Design and Frequency Band Allocation for Energy-efficient and Fair Communication: A Deep Reinforcement Learning Approach," *IEEE Transactions on Wireless Communications*, vol. 19, no. 12, pp. 7796–7809, Dec. 2020.
- [30] C. You and R. Zhang, "3D Trajectory Optimization in Rician Fading for UAV-enabled Data Harvesting," *IEEE Transactions on Wireless Communications*, vol. 18, no. 6, pp. 3192–3207, Jun. 2019.
- [31] Y. Zeng, X. Xu, and R. Zhang, "Trajectory Design for Completion Time Minimization in UAV-enabled Multicasting," *IEEE Transactions on Wireless Communications*, vol. 17, no. 4, pp. 2233–2246, Apr. 2018.
- [32] C. Zhan, Y. Zeng, and R. Zhang, "Trajectory Design for Distributed Estimation in UAV-enabled Wireless Sensor Network," *IEEE Transactions on Vehicular Technology*, vol. 67, no. 10, pp. 10 155–10 159, Oct. 2018.
- [33] W. Wang, X. Li, R. Wang, K. Cumanan, W. Feng, Z. Ding, and O. A. Dobre, "Robust 3D-trajectory and Time Switching Optimization for Dual-UAV-enabled Secure Communications," *IEEE Journal on Selected Areas in Communications*, vol. 39, no. 11, pp. 3334–3347, Nov. 2021.
- [34] Q. Wu, Y. Zeng, and R. Zhang, "Joint Trajectory and Communication Design for Multi-UAV Enabled Wireless Networks," *IEEE Transactions on Wireless Communications*, vol. 17, no. 3, pp. 2109–2121, Mar. 2018.
- [35] J. Li, H. Zhao, H. Wang, F. Gu, J. Wei, H. Yin, and B. Ren, "Joint Optimization on Trajectory, Altitude, Velocity, and Link Scheduling for Minimum Mission Time in UAV-Aided Data Collection," *IEEE Internet of Things Journal*, vol. 7, no. 2, pp. 1464–1475, Feb. 2020.
- [36] J. Gong, T.-H. Chang, C. Shen, and X. Chen, "Flight Time Minimization of UAV for Data Collection Over Wireless Sensor Networks," *IEEE Journal on Selected Areas in Communications*, vol. 36, no. 9, pp. 1942–1954, Sep. 2018.
- [37] K. Li, W. Ni, E. Tovar, and A. Jamalipour, "On-Board Deep Q-Network for UAV-Assisted Online Power Transfer and Data Collection," *IEEE Transactions on Vehicular Technology*, vol. 68, no. 12, pp. 12 215–12 226, Dec. 2019.
- [38] Z. Wang, R. Liu, Q. Liu, J. S. Thompson, and M. Kadoch, "Energy-Efficient Data Collection and Device Positioning in UAV-Assisted IoT," *IEEE Internet of Things Journal*, vol. 7, no. 2, pp. 1122–1139, Feb. 2019.
- [39] H. Huang, Y. Yang, H. Wang, Z. Ding, H. Sari, and F. Adachi, "Deep Reinforcement Learning for UAV Navigation Through Massive MIMO Technique," *IEEE Transactions on Vehicular Technology*, vol. 69, no. 1, pp. 1117–1121, Nov. 2019.
- [40] C. Zhan and Y. Zeng, "Aerial–Ground Cost Tradeoff for Multi-UAV-Enabled Data Collection in Wireless Sensor Networks," *IEEE Transactions on Communications*, vol. 68, no. 3, pp. 1937–1950, Mar. 2020.
- [41] M. Samir, C. Assi, S. Sharafeddine, D. Ebrahimi, and A. Ghayeb, "Age of Information Aware Trajectory Planning of UAVs in Intelligent Transportation Systems: A Deep Learning Approach," *IEEE Transactions on Vehicular Technology*, vol. 69, no. 11, pp. 12 382–12 395, Nov. 2020.
- [42] K. K. Nguyen, T. Q. Duong, T. Do-Duy, H. Claussen, and L. Hanzo, "3D UAV Trajectory and Data Collection Optimisation Via Deep Reinforcement Learning," *IEEE Transactions on Communications*, vol. 70, no. 4, pp. 2358–2371, Apr. 2022.
- [43] Y. Hu, M. Chen, W. Saad, H. V. Poor, and S. Cui, "Distributed Multi-agent Meta Learning for Trajectory Design in Wireless Drone Networks," *IEEE Journal on Selected Areas in Communications*, vol. 39, no. 10, pp. 3177–3192, Oct. 2021.
- [44] H. Tang, Q. Wu, J. Xu, W. Chen, and B. Li, "A Novel Alternative Optimization Method for Joint Power and Trajectory Design in UAV-Enabled Wireless Network," *IEEE Transactions on Vehicular Technology*, vol. 68, no. 11, pp. 11 358–11 362, Nov. 2019.
- [45] S. Kouroshnezhad, A. Peiravi, M. S. Haghghi, and A. Jolfaei, "Energy-efficient Drone Trajectory Planning for the Localization of 6G-enabled IoT Devices," *IEEE Internet of Things Journal*, vol. 8, no. 7, pp. 5202–5210, Apr. 2021.
- [46] R. I. Bor-Yaliniz, A. El-Keyi, and H. Yanikomeroglu, "Efficient 3-D Placement of an Aerial Base Station in Next Generation Cellular Networks," in *Proceeding of 2016 IEEE International Conference on Communications (ICC)*, pp. 1–5.
- [47] E. Kalantari, H. Yanikomeroglu, and A. Yongacoglu, "Wireless Networks With Cache-enabled and Backhaul-limited Aerial Base Stations," *IEEE Transactions on Wireless Communications*, vol. 19, no. 11, pp. 7363–7376, Nov. 2020.
- [48] E. W. Dijkstra *et al.*, "A note on two problems in connexion with graphs," *Numerische Mathematik*, vol. 1, no. 1, pp. 269–271, Jun. 1959.
- [49] X. Zhong, Y. Huo, X. Dong, and Z. Liang, "QoS-Compliant 3-D Deployment Optimization Strategy for UAV Base Stations," *IEEE Systems Journal*, vol. 15, no. 2, pp. 1795 – 1803, Jun. 2021.